Effect of 3-D fields on divertor detachment and associated pedestal profiles in NSTX H-mode plasmas

J-W. Ahn[1], R. Maingi[1], A.G. McLean[1], J.M. Canik[1], A. Diallo[2], T.K. Gray[1], M. Jaworski[2], B. LeBlanc[2], A.L. Roquemore[2], V.A. Soukhanovskii[3], K. Tritz[4], A. Loarte[5]

[1]*Oak Ridge National Laboratory, Oak Ridge, TN 37831, USA*
[2]*Princeton Plasma Physics Laboratory, Princeton, NJ 08543, USA*
[3]*Lawrence Livermore National Laboratory, Livermore, CA 94551, USA*
[4]*Johns Hopkins University, Baltimore, MD 21218, USA*
[5]*ITER Organization, St. Paul-lez-Durance, France*

1. Introduction

The effect of externally applied 3-D magnetic perturbations on the divertor heat and particle flux profiles has been actively studied in various tokamaks, for example in DIII-D [1] and NSTX [2,3]. These phenomena are directly related with the 'strike point (SP) splitting' caused by the 3-D magnetic field perturbations to the plasma edge [4]. As ITER is considering the use of 3-D magnetic fields for the control of ELM transient heat loads, a detailed understanding of the physical mechanism leading to the ELM suppression as well as the changes to the edge transport associated with the application of 3-D fields is necessary. Partial detachment is the divertor operation regime selected for ITER high fusion performance operation, as it allows control of heat fluxes to the divertor and erosion at the material surface during the stationary phase to values acceptable for the PFC operation lifetime. It is essential that the two schemes be compatible with each other. Thus we have investigated the effect of applied 3-D fields on the divertor detachment and its relation to the pedestal profiles in National Spherical Torus Experiment (NSTX).

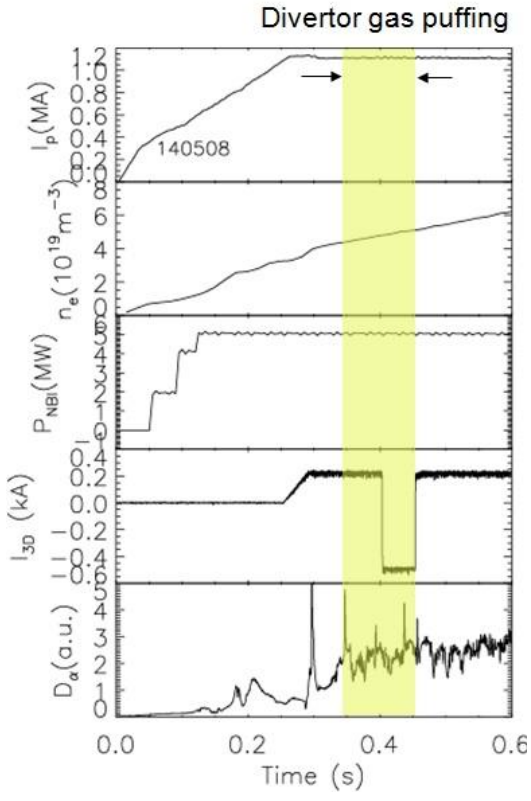

Fig. 1 Time trace of several discharge parameters. Divertor gas injection (D_2) was made for t=350-450ms period (shaded area) and the 3-D fields (n=3) were applied for 50ms from t=400ms (4th panel from the top)

2. Experimental setup and measurement technique

Six midplane coils located close to the outer vacuum vessel are used to apply magnetic perturbations in NSTX. The divertor gas injection system was used to induce divertor detachment. The amount of puffed gas was varied to change the divertor plasma condition through high recycling and partial detachment. The surface temperature measurements for the lower divertor target are made with a high speed (1.6kHz) dual-band infrared (IR) camera [5,6] with 5-7mm spatial resolution. A 2-D heat conduction code, THEODOR [7], is used to calculate the divertor heat flux profile from the surface temperature. D_α emission at the lower divertor target is recorded by a 1-D CCD camera [8] at a 2kHz rate and with sub-mm spatial resolution. Note that we are using the D_α emission as a proxy for the particle flux in attached plasmas. Two poloidal arrays of ultrasoft x-ray (USXR) diagnostic [9] (16 channels each) recorded line of sight integrated X-ray emissions ($dI = \varepsilon dl$) with spectral region 10-100 Å, covering from the plasma edge to the core region. A flush mounted Langmuir probe (LP) with sweeping frequency of 100Hz was also used to monitor divertor plasma conditions such as particle flux (I^+_{sat}), electron temperature (T_e) and density (n_e), and floating potential (V_f) [10]. Figure 1 shows the time trace of several discharge parameters.

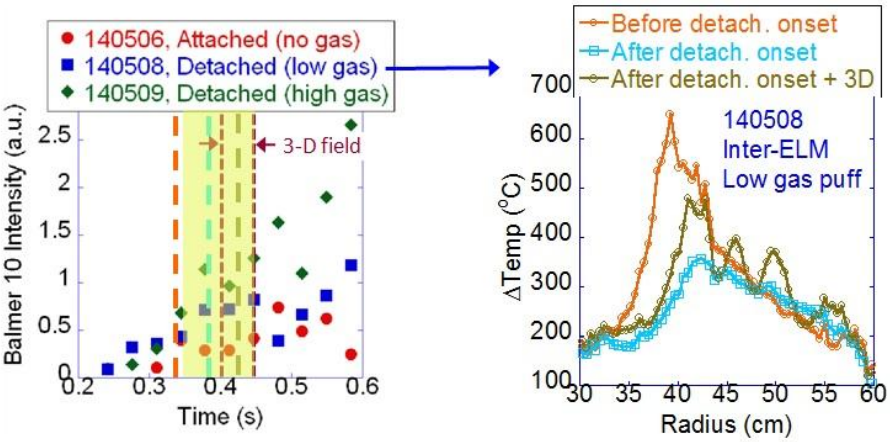

Fig. 2 Time trace of Balmer 10 line intensities (left) and the measured divertor surface temperature profiles by the IR camera (right) for different gas injection rates. Gas puffing was for t=350-450ms (yellow shaded).

3. Data analysis and interpretation

Divertor plasma detachment is generally signified by a substantial reduction of measured particle flux to the divertor surface and is also accompanied by heat flux reduction. The dual-band IR data shows that the peak in the heat flux profile disappears during the divertor gas injection, making the heat flux profile more flattened. This is a typical signature of partial detachment, *i.e.* detachment only near the strike point, and LP data also showed that the measured particle flux decreased during the gas puffing period. The measured Balmer 10 line intensities at the divertor surface (left plot of figure 2) rise for higher gas puffing rate and

this indicates higher degree of detachment. For lower gas puffing case, the flattened surface temperature profile by detachment becomes peaked again when the 3-D fields (n=3) were applied, which indicates that the divertor plasma reattached. However, divertor plasma with higher gas puff rates remained detached even with the 3-D field application.

We investigated the effect of divertor detachment and the applied 3-D fields on the mid-plane T_e, n_e, T_i, and the toroidal rotation velocity (v_t) profiles. It is found that detachment reduces pedestal T_e most clearly, while n_e reduction was less significant, and the pedestal T_i and v_t also decreased. This drop becomes stronger with increasing gas puff rate. During the re-attachment by the 3-D field application with the lower gas puff rate, the pedestal T_e profile shows a clear increase, while the pedestal density changes little (figure 3). Thus the pedestal pressure increases and it is consistent with the observed increase of the plasma stored energy, w_{mhd}=230kJ → 245kJ, calculated from EFIT. It is interesting to note that T_i profile showed no change and the v_t profile continued to decrease during the plasma re-attachment (see figure 3). This data implies that the reattachment may be dominated by the change in the electron transport. For the higher gas puff case, the 3-D fields had no impact and the pedestal profiles remained decreased, which is consistent with the continued divertor detachment during the 3-D fields application phase. Figure 4 shows the temporal evolution of the line integrated USXR signals for the cases with and without detachment and the 3-D field application. Channel #0 represents the outer most edge channel and #15 is for the most core channel. It is seen that a steep gradient in the edge region exists if there is no divertor gas puff. This gradient disappears as the detachment sets on and the temporal evolution of the channel signals indicates that the flattening propagates from the edge toward the core region (top right plot in figure 4). Curiously, for the re-attachment case with the lower gas puff, the applied 3-D field restored the edge gradient and again the change propagated from the edge toward the core

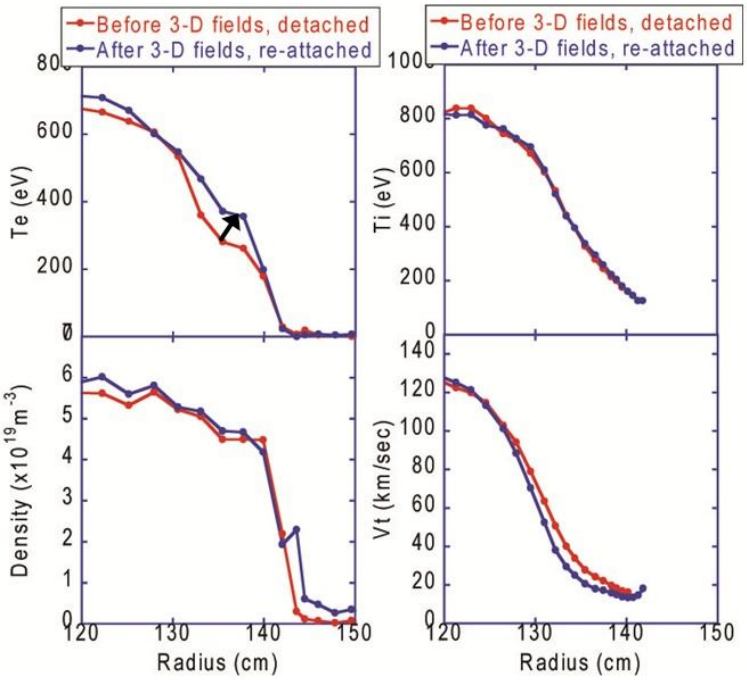

Fig. 3 Temporal evolution of T_e, n_e, T_i, and v_t profiles before (red) and after (blue) the 3-D fields application during the divertor detachment with a lower gas puff rate.

(bottom left). It may be possible that this restoration is related to the observed pedestal T_e increase (see figure 3). The edge gradient remained decreased with high gas puff rate during the 3-D field application phase (bottom right) and it is consistent with the observation that the divertor plasma remained detached as described above. Without any gas puff, the 3-D field is observed to cut off only the very edge emissions (top left plot). In conclusion, the fact that higher gas puff rate prevented the detached plasma from reattaching with applied 3-D fields indicates that the 3-D field application and the divertor detachment can be compatible with each other.

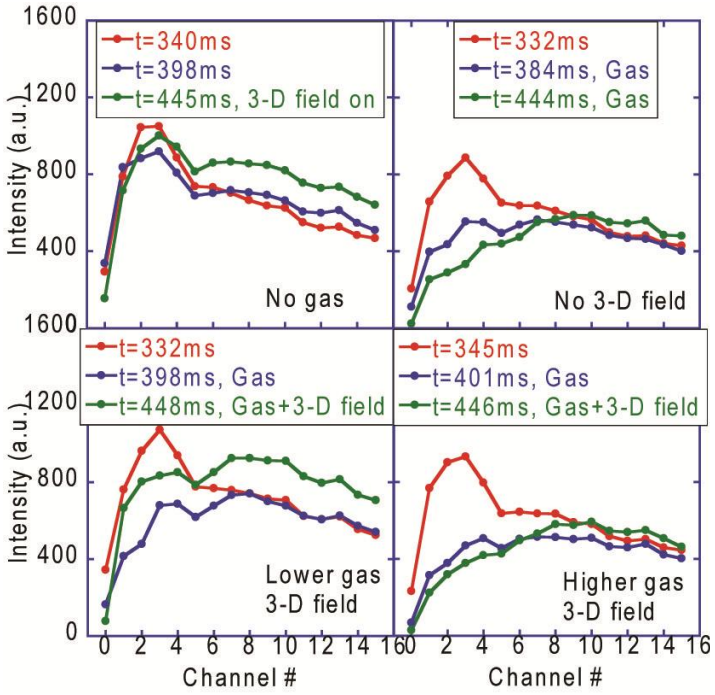

Fig. 4 Line integrated USXR channel signals with and without divertor gas puff and 3-D field application.

Acknowledgements

This work was funded by the US Department of Energy, contract numbers DE-AC05-000R22725, DE-AC02-09CH11466, DE-AC52-07NA27344, and DE-AC02-09CH11466. We thank A. Herrmann for use of the THEODOR heat conduction code.

References

[1] M. W. Jakubowski, T. E. Evans, M. E. Fenstermacher, *et al*, Nucl. Fusion **49** (2009) 095013

[2] J-W. Ahn, J. M. Canik, R. Maingi, *et al*, Nucl. Fusion **50** (2010), 045010

[3] J-W. Ahn, R. Maingi, J. M. Canik, *et al*, Phys. Plasmas **18** (2011), 056108

[4] T. E. Evans, R. K. W. Roeder, J. A. Carter, B. I. Rapoport, M. E. Fenstermacher and C. J. Lasnier, J. Phys : Conf. Ser. **7** (2005) 174-90

[5] J-W. Ahn, R. Maingi, D. Mastrovito, and A. L. Roquemore, Rev. Sci. Instrum. **81** (2010) 023501

[6] A. McLean, J-W. Ahn, R. Maingi, etc, 'A dual-band adaptor for infrared imaging', submitted to Rev. Sci. Instrum. (2011)

[7] A. Herrmann, W. Junker, K. Gunther, *et al*, Plasma Phys. Control. Fusion **37** (1995) 17

[8] V. A. Soukhanovskii, A. L. Roquemore, C. H. Skinner, *et al*, Rev. Sci. Instrum. **74** (2003) 2094

[9] D. Stutman, et al., Rev. Sci. Instrum. **68** (1999) 572

[10] M. Jaworski, et al, Rev. Sci. Instrum. **81** (2010) 10E130